Available online at www.sciencedirect.com
SCIENCE DIRECT®
Catalysis Today 89 (2004) 389–403
CATALYSIS TODAY
www.elsevier.com/locate/cattod

Syngas production by biomass gasification using $Rh/CeO_2/SiO_2$ catalysts and fluidized bed reactor

Keiichi Tomishige*, Mohammad Asadullah, Kimio Kunimori

Institute of Materials Science, University of Tsukuba, 1-1-1 Tennodai, Tsukuba 305-8573, Ibaraki, Japan

Received 11 July 2003; received in revised form 6 December 2003; accepted 5 January 2004

Available online 22 April 2004

Abstract

We have been developed novel catalysts for gasification of biomass with much higher energy efficiency than conventional methods (non-catalyst, dolomite, commercial steam reforming Ni catalyst). From the result of the gasification of cellulose over novel $Rh/CeO_2/SiO_2$ catalysts, it is found that the gasification process consists of the reforming of tar and the combustion of solid carbon. We also tested novel $Rh/CeO_2/SiO_2$ in the gasification with air, pyrogasification, and steam reforming of cedar wood. As a result, $Rh/CeO_2/SiO_2$ gave higher yield of syngas than the conventional steam reforming Ni catalyst. Furthermore, we compared the performance between single and dual bed reactors. Single bed reactor was effective in the gasification of cedar, however, it was not suitable for the gasification of rice straw since a rapid deactivation was observed. Gasification of rice straw, jute stick, baggase using the fluidized dual-bed reactor and $Rh/CeO_2/SiO_2$ was also investigated. Especially, the catalyst stability in the gasification of rice straw clearly was enhanced by using the fluidized dual bed reactor.
© 2004 Elsevier B.V. All rights reserved.

Keywords: Biomass; Cellulose; Gasification; Synthesis gas; Fluidized-bed; Rhodium; Cerium oxide

1. Introduction

Regulations against poisonous components in the exhaust gas such as SO_x, NO_x and particulate matter (PM) and against sulfur content in transportation fuels has been strengthened. From this point of view, the diesel engine has a serious problem. This is because 75% of the automobile-origin NO_x and almost 100% automobile-origin PM. On the other hand, the diesel engine has an advantage in higher thermal efficiency compared to the gasoline engine. Therefore more attention is paid to clean diesel fuels. One possible solution is synthetic fuels such as Fischer–Tropsch oil and dimethyl ether because it is known that the synthetic fuels can reduce the emission of NO_x, PM and SO_x [1]. The synthetic fuels can be synthesized from syngas, which is supplied by coal gasification and steam reforming of methane in an industrial scale at present. Furthermore, when syngas is produced from biomass, the emission of CO_2 can be decreased since from the "carbon neutral" point of view [2].

The gasification of biomass at around 1073–1223 K to syngas (H_2+CO) can potentially be used either as a gaseous fuel for power generation or as a feedstock for the synthesis of clean transportation fuels or many other chemicals. The formation of tar and char in the gasification process is the most severe problems [3–14]. It is known that an entrained bed gasification method can reduce the tar remarkably, therefore the technology is being developed as a project supported by NEDO in Japan, although it is necessary to make wood biomass to small powder [15]. The vaporized tars can condense either onto wall surfaces or into aerosols of small droplets when they were cooled. In terms of the utilization of produced gas to gas turbines or catalytic conversion of syngas to useful liquid fuels or chemicals, the droplets of tars deposit on either the turbine system that cause mechanical problems or on the catalyst surface that cause the catalyst deactivation [12–14]. Therefore most of the researches have focused on the extensive cleanup of the product gas [16–18].

According to the literature, the tar removal from the product gas stream by catalytic cracking is one of the most promising methods and it has been investigated for more

* Corresponding author. Tel.: +81-29-853-5030; fax: +81-29-853-5030.
E-mail address: tomi@tulip.sannet.ne.jp (K. Tomishige).

0920-5861/$ – see front matter © 2004 Elsevier B.V. All rights reserved.
doi:10.1016/j.cattod.2004.01.002

than two decades [19–28]. The studies on the catalytic gasification of biomass include the use of catalyst either in the gasifier itself or in separate reactors downstream from the gasifier [29]. Some nickel-based catalysts [30–37], dolomite [38] and olivine [39] catalysts have been found to be active catalysts for tar cracking in the primary reactor within the temperature range of 1073–1173 K for dolomite and olivine, and 973–1073 K for nickel-based catalysts. However, it has been reported that the Ni-based catalysts were deactivated significantly by carbon deposition on the catalyst surface [30–33,40,41].

Recently we have found that Rh/CeO_2 exhibited the high activity in cellulose gasification. The CeO_2 supported Rh catalyst efficiently converted the total carbon in the cellulose to gas products even at 823 K [42,43]. However, the sintering of CeO_2 and the catalyst deactivation was observed. And then, in order to inhibit the sintering of CeO_2, CeO_2 was loaded on other supports with high surface area and inert properties. We have developed stable $Rh/CeO_2/SiO_2$ catalyst for the gasification of cellulose [44–50]. Furthermore, we tested the performance of $Rh/CeO_2/SiO_2$ catalyst in the gasification of cedar wood [51–57]. In this review, we evaluate this catalytic gasification in terms of the cold gas efficiency and the role of catalyst components is discussed. In addition, we also tested the $Rh/CeO_2/SiO_2$ in the gasification of other biomasses than cedar wood such as jute, rice straw, and baggase. Especially, we also developed the dual bed reactor whose function was the separation of char and ash from volatile tar.

2. Experimental

2.1. Catalyst preparation

The catalysts used in this investigation are $Rh/CeO_2/SiO_2$ with 1.2×10^{-4} mol Rh/g of catalyst and various contents of CeO_2, commercial steam reforming Ni catalyst (G-91, TOYO CCI, catalyst composition: 14 mass% Ni, 65–70 mass% Al_2O_3, 10–14 mass% CaO, and 1.4–1.8 mass% K_2O), and dolomite (21.0 mass% MgO, 30.0 mass% CaO, 0.7 mass% SiO_2, 0.1 mass% Fe_2O_3, and 0.5 mass% Al_2O_3). The dolomite was calcined at 773 K for 3 h before reaction. The CeO_2/SiO_2 was prepared by the incipient wetness method using the aqueous solution of $Ce(NH_4)_2(NO_3)_6$ and SiO_2 (Aerosil, 380 m^2/g). The loading of CeO_2 on SiO_2 was in the range of 10–80 mass%. After loading, it was dried at 383 K for 12 h and then the calcination at 773 K for 3 h under air atmosphere was carried out. After that, the Rh was loaded on CeO_2/SiO_2 by impregnation of the support with acetone solution of $Rh(C_5H_7O_2)_3$. The acetone solvent was then evaporated at around 333 K with constant stirring, and the catalyst was dried at 383 K for 12 h. The final catalyst was pressed, crushed and sieved to 45–150 μm particle size. The mass% of CeO_2 in the $Rh/CeO_2/SiO_2$ is denoted in the parentheses, such as $Rh/CeO_2/SiO_2(60)$. In each run, 3 g of catalyst was used and pretreated by a hydrogen flow at 773 K for 0.5 h. After this hydrogen reduction, the reactor was purged with nitrogen sufficiently at 773 K. At this point, adsorbed hydrogen on the catalyst surface was desorbed completely. In the activity test, chemisorbed hydrogen is not necessary to consider at all. The fresh (after H_2 treatment) and used catalysts were characterized by a Brunauer–Emmett–Teller (BET) analysis. Chemisorption experiments were carried out in high-vacuum system by volumetric methods. Research grade gas (H_2: 99.99%, Takachiho Trading Co. Ltd.) was used without further purification. Before H_2 adsorption measurement, the catalysts were treated in H_2 at 773 K for 0.5 h. H_2 adsorption was performed at room temperature. Gas pressure at adsorption equilibrium was about 1.1 kPa. The sample weight was about 0.2 g. The dead volume of the apparatus was about 60 ml.

2.2. Apparatus for the activity test using fluidized bed reactors

The sketch diagram of the single bed reactor is shown in Fig. 1. The reactor was made of quartz glass. An inner

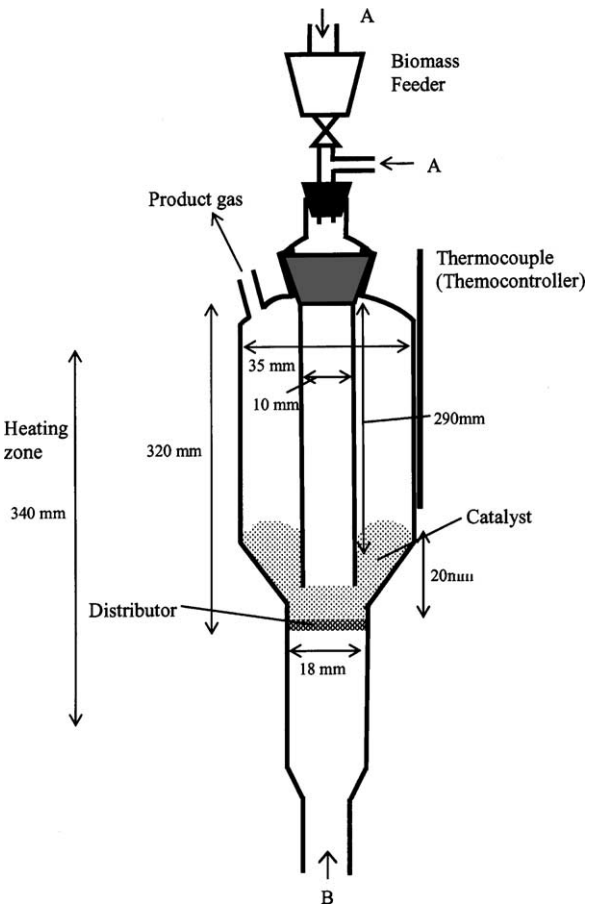

Fig. 1. Schematic diagram of the single-bed reactor. Gasification with air A: N_2 + biomass, B: $O_2 + N_2$; pyrogasification A: N_2 + biomass, B: N_2; steam reforming A: N_2 + biomass, B: $H_2O + N_2$; solid carbon (char + coke) estimation A: N_2, B: O_2.

tube was inserted from the top. Cellulose and biomass were supplied from the top of the reactor together with N_2 from the port A. The biomass feeder consisted of a glass vessel with a small pore at the bottom and it was vibrated by the vibrator and the feeding rate was controlled by the vibrating rate. The gasifier was composed of a fluidized bed section at the middle of the reactor. In the gasification of biomass with oxygen, O_2 and N_2 were supplied from the port B. In the pyrogasification, N_2 was supplied from the port B. In the case of steam reforming of biomass, N_2 and steam was supplied from the port B. The microfeeder was used for steam feeding. The product gas was collected and analyzed by gas chromatography (GC). The concentration of CO, CO_2 and CH_4 products was determined by FID-GC equipped with a methanator using a stainless steel column packed with Gasukuropack 54 and the concentration of hydrogen was determined by TCD-GC using a stainless steel column packed with a molecular sieve 13×. The flowing rate of the effluent gas out of the reactor was measured by a soap membrane meter. The amount of solid carbon (coke on the catalyst and char) was determined by the total amount of gas (mainly CO_2) formed under the air flowing at the reaction temperature after we stopping the feeding of biomass and cellulose. These activity tests were carried out under atmospheric pressure by using 3 g of catalyst in the fluidized bed.

Fig. 2 shows the sketch diagram of the dual bed reactor, and this consisted of two fluidized-bed sections. First section was located at the bottom of the conical part on the outer quartz tube and the other one was at the bottom of the inner tube. The catalyst particles were placed in the fluidized-bed section of inner tube. The biomass was fed from the feeder by vibrating with an electric vibrator and transported through the side tube under nitrogen flowing. In the case of this dual-bed gasifier, oxygen was supplied through a capillary tube which was inserted to the inner tube from the top of the fluidized-bed reactor. At first, biomass was pyrolyzed in the outer tube to form the tar and char mainly. The char accumulated in the conical bed section and the tar reached the catalyst-bed and took part in the reforming reaction. In contrast, all the biomass-derived products in the feeding tube go to the catalyst-bed in the single-bed type.

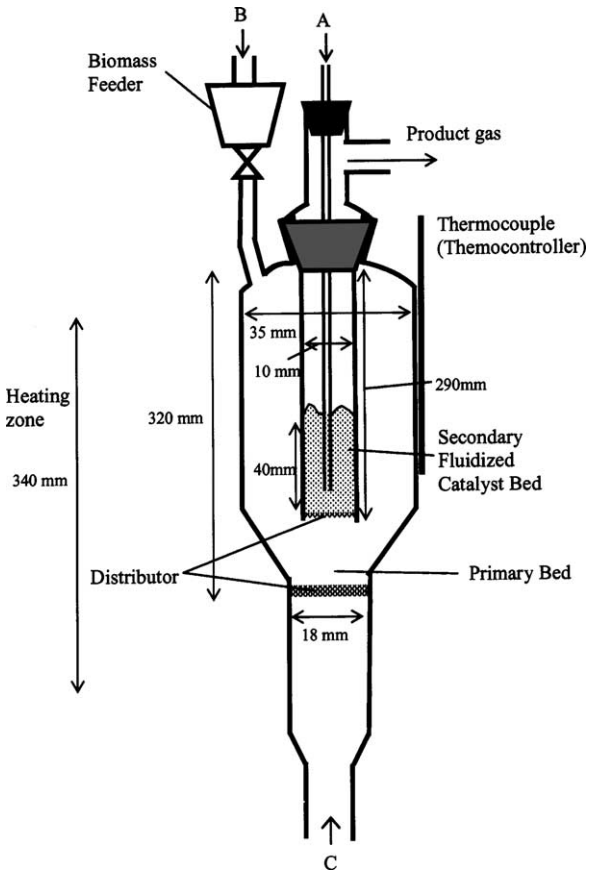

Fig. 2. Schematic diagram of the dual-bed reactor. Activity test of biomass gasification A: O_2, B: N_2 + biomass, C: N_2; coke estimation A: O_2, B: N_2, C: N_2; char estimation A: N_2, B: O_2, C: O_2.

2.3. Data processing

The analysis of the product gases were carried out in the similar way to that in the single-bed reactor. In the non-catalyzed and dolomite-catalyzed reactions, a small amount of C_2 product was formed. However, in other experiments, amount of C_2 product was below the detection limit. The formation rate of the gas products was calculated from the GC analysis of the gas flowing out of the reactor in the unit of μmol/min. The carbon-based conversion to gas (C-conversion) was calculated by "$A/B \times 100$", where A represents the formation rate of $CO + CO_2 + CH_4$ and B represents the total carbon supplying rate of biomass or cellulose. The C-conversion listed in the tables is an average one during the reaction (15–25 min). The yield of solid carbon (coke + char) was calculated by (total amount of CO_2 + CO)/(total carbon amount in fed biomass) × 100. It is difficult to distinguish between char and coke on the catalyst in the case of single bed reactor. Therefore, the yield of solid carbon in the single-bed system corresponds to the sum of char and coke. In the case of the dual-bed gasifier, first the coke deposited on the catalyst surface was determined by measuring the CO_2 derived from the coke by burning it with oxygen. After that, the amount of char accumulated in the pyrolysis zone was determined by burning. In this case, oxygen was introduced from the top and bottom of the outer quartz tube. The tar yield was estimated by (100 − C-conversion (% C) − solid carbon (char + coke) yield (% C)). The feeding rate of biomass or cellulose, N_2, and air are described in each result. Equivalence ratio (ER) can be calculated by (supplied oxygen weight)/(dry biomass weight)/(stoichiometric oxygen weight/dry biomass weight for complete combustion).

Energy efficiency of cellulose and biomass gasification can be estimated on the basis of cold gas efficiency. The cold gas efficiency was calculated by the ratio of heat value of biomass combustion to that of produced gas. In this calculation, the heat energy supplied from the furnace is neglected.

Table 1
Properties of various biomasses

	Cedar wood	Jute stick	Baggase	Rice straw
Particle size (mm)	0.1–0.3	0.1–0.3	0.1–0.3	0.1–0.3
Moisture content (wt.%)	10.0	3.0	5.0	11.4
Heating value (HHV) (kcal/kg)	4570	4699	4555	3080
Ultimate analysis (dry basis, wt.%)				
C	51.10	49.79	48.58	36.9
H	5.90	6.02	5.97	4.7
O	42.50	41.37	38.94	32.5
N	0.12	0.19	0.2	0.3
Cl	0.01	0.05	0.05	0.08
S	0.02	0.05	0.05	0.06
Proximate analysis (dry basis)				
Volatile fraction (wt.%)	69	77	69	49
Fixed carbon (wt.%)	30.7	22.4	29.7	28.4
Ash (wt.%)	0.3	0.6	1.3	22.6

2.4. Cellulose and biomass

Cellulose was purchased from Merk and the particle size was 100–160 μm. Various kinds of biomass such as cedar wood (Japan), jute stick (Bangladesh), baggase (Bangladesh), and rice straw (Japan) were used for the gasification. The moisture contents were cedar wood 10%, jute stick 5%, baggase 3%, and rice straw 11.4%, respectively. The biomass was processed with a ball mill to about 0.1–0.3 mm size. The analysis of these biomasses was carried out by Japan Institute of Energy. The properties of different biomass are summarized in Table 1.

3. Results and discussion

3.1. Role of CeO_2 in $Rh/CeO_2/SiO_2$ for the gasification of cellulose

Catalyst performance of $Rh/CeO_2/SiO_2$ catalysts with various CeO_2 contents in the gasification of cellulose using the single-bed reactor is listed in Table 2. The dependence of the formation rate of the products on reaction time is not shown here, the stable activity was observed during the 25 min reaction over each catalyst. At higher reaction temperature, the level of C-conversion approached 100%. In this case, the formation rate of products was similar over all the catalysts except Rh/SiO_2, on which C-conversion did not reach about 100%. This is because the gas composition can be determined by the reaction equilibrium. In contrast, the difference in C-conversion and formation rate among the catalysts became larger at lower reaction temperature. This indicates that the gas composition is controlled by reaction rate on each catalyst. Therefore, if we like to compare the catalyst performance and the reaction rate, we should use the data at lower reaction temperature. Dependence of C-conversion and cold gas efficiency in the gasification of cellulose on CeO_2 content in $Rh/CeO_2/SiO_2$ catalysts at 823 K is shown in Fig. 3. There was a maximum in the C-conversion and the cold gas efficiency at 35 mass% CeO_2 content. BET surface area decreased with increasing CeO_2 content in the catalyst. Since Rh/SiO_2 gave the high yield of tar and solid carbon, it showed low performance of Rh/SiO_2 in the gasification of cellulose. However, only 10 mass% CeO_2 addition decreased the yield of tar and solid carbon drastically, and this indicates that CeO_2 promoted the gasification reaction significantly. On the other hand, the addition of CeO_2 decreased the catalyst surface area, and this can make the particle size of Rh metal large and reduce the activity. This means that the additive effect of CeO_2 has both positive and negative aspects. This can interpret the maximum of the C-conversion and the cold gas efficiency.

Furthermore Fig. 4 shows the relation between the formation rate of products and the amount of solid carbon and tar in the gasification of cellulose over $Rh/CeO_2/SiO_2$ at 823 K. From the relation between solid carbon yield and CO_2 formation rate, the decrease of solid carbon yield caused the increase of CO_2 formation rate. One percent of solid carbon yield corresponds to 31 μmol/min CO_2 formation rate from

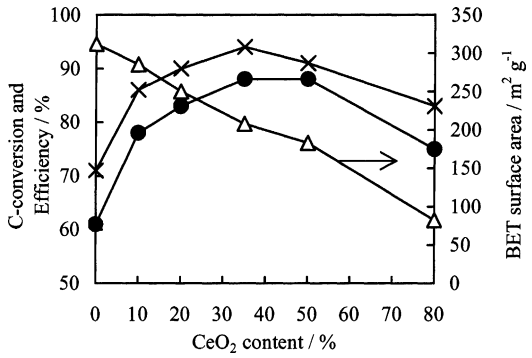

Fig. 3. Dependence of C-conversion (×), cold gas efficiency (●) in the gasification of cellulose at 823 K and catalyst surface area (△) on CeO_2 content in $Rh/CeO_2/SiO_2$ using single-bed reactor. Reaction conditions are the same in Table 2.

Table 2
Performance of $Rh/CeO_2/SiO_2$ catalysts in the gasification of cellulose using the single-bed reactor[a]

Catalyst	T (K)	Formation rate (μmol/min)						C-conversion (% C)[b]	Solid carbon (%C)[c]	Tar (% C)[d]	Efficiency (%)[e]
		CO	H_2	CH_4	CO_2	C2	H_2/CO				
Rh/SiO_2	823	1194	1287	222	820	0	1.1	71	12	17	61
	873	1479	1514	310	767	0	1.0	81	12	7	76
	973	2169	2039	198	506	0	0.9	91	5	4	92
$Rh/CeO_2/SiO_2$(10)	823	1633	1705	233	840	0	1.1	86	8	6	78
	873	1591	1460	536	814	0	0.9	93	3	4	90
	923	2186	2032	366	530	0	0.9	98	2	0	103
	973	2201	2013	315	600	0	0.9	99	1	0	99
$Rh/CeO_2/SiO_2$(20)	823	1285	1359	542	1004	0	1.1	90	5	1	83
	873	1750	1890	540	735	0	1.1	96	4	0	102
	923	2082	1929	468	535	0	0.9	98	2	0	105
	973	2255	1994	315	529	0	0.9	99	1	0	100
$Rh/CeO_2/SiO_2$(35)	823	1250	1286	653	1050	0	1.1	94	4	2	88
	873	1617	1666	470	966	0	1.0	97	3	0	91
	923	2254	2061	172	644	0	0.9	99	1	0	93
	973	2279	2357	211	615	0	1.0	99	1	0	101
$Rh/CeO_2/SiO_2$(50)	823	1195	1250	685	925	0	1.1	91	5	4	88
	873	1645	1642	516	905	0	1.0	97	3	0	94
	923	2029	1977	394	659	0	0.9	98	2	0	100
	973	2399	2218	210	607	0	0.9	99	1	0	101
$Rh/CeO_2/SiO_2$(80)	823	1112	1126	542	954	0	1.0	83	5	12	75
	873	1476	1466	534	875	0	1.0	92	4	4	88
	923	2223	1951	339	508	0	0.9	98	2	0	100

[a] Conditions: cellulose, 85 mg/min (C, 3148 μmol/min; H, 5245 μmol/min; O, 2623 μmol/min); air, 50 cm^3/min (O_2 417 μmol/min); N_2, 50 cm^3/min; total pressure 0.1 MPa, catalyst weight, 3 g; particle size of catalyst, 150–250 μm, H_2 reduction at 773 K for 0.5 h.
[b] C conversion to gas = {(formation rate of $CO + CO_2 + CH_4$)/C-feeding rate} × 100.
[c] Char (% C) = ($CO + CO_2$ formation amount after stopping cellulose feeding/total C feeding) × 100.
[d] Tar (% C) = 100 − (C conversion (% C) + solid carbon (% C)).
[e] Efficiency: cold gas efficiency.

the calculation. This can explain the relation between the solid carbon yield and CO_2 formation rate. From the relation between tar yield and $CO+CH_4$ formation rate, the decrease of tar yield caused the increase of $CO+CH_4$ formation rate. In the case of tar yield, 1% also corresponds to 31 μmol/min $CO+CH_4$ formation rate. This also can explain the relation between the tar yield and $CO + CH_4$ formation rate. CO and CH_4 are the products in the reforming of hydrocarbons since CH_4 is formed by CO hydrogenation ($CO + 3H_2 \rightarrow CH_4+H_2O$). This reaction is reversible. The reverse reaction is steam reforming of methane($CH_4 + H_2O \rightarrow CO + 3H_2$) and this is a highly endothermic reaction. Therefore the partial pressure of methane decreases at higher reaction temperature when the reaction reaches the equilibrium level. It is observed that this behavior becomes more significant at higher reaction temperature in Table 2. This suggests that CO hydrogenation and methane reforming reaction can proceed on the catalyst surface. On the other hand, water gas shift reaction ($CO + H_2O \rightarrow CO_2 + H_2$) is also reversible reaction and it is thought that this reaction can proceed on the catalyst surface. This indicates that various kinds of reaction proceed on the catalyst surface, and the formation rate of products can be influenced by all these reactions. Therefore, it is necessary to simulate the phenomenon in order to elucidate the detail. However, it is possible to discuss the tendency of the behavior. The relation between the formation rate of $CO + CH_4$ and tar yield suggests that tar is removed by catalytic reforming. The relation between the formation rate of CO_2 and solid carbon yield suggests that solid carbon is removed by the combustion.

On the basis of the above suggestions, we like to discuss what occurs in the reactor during the gasification of cellulose. In the feeding line of the reactor, cellulose can reach a heated region before the contact with the catalyst particles, and it is thermally decomposed to the tar, char, steam, and gas products since the carrier gas of biomass is nitrogen. This can be related to the non-catalytic gasification of cellulose as shown in Table 3. After this, the pyrolyzed products including the volatile tar and solid carbon are introduced to the fluidized catalyst bed and they are interacted with the catalyst particles in the lower part of the catalyst bed.

Under our reaction conditions, ER is as low as 0.3, it is expected that there are two regions in the fluidized bed reactor. In one region, O_2 is present and the atmosphere is oxidative. In the other region, O_2 is absent and the atmosphere is reductive. Since oxygen is introduced from the bottom of the reactor, it is thought that first region is in the lower part of the catalyst bed and second region is in the higher

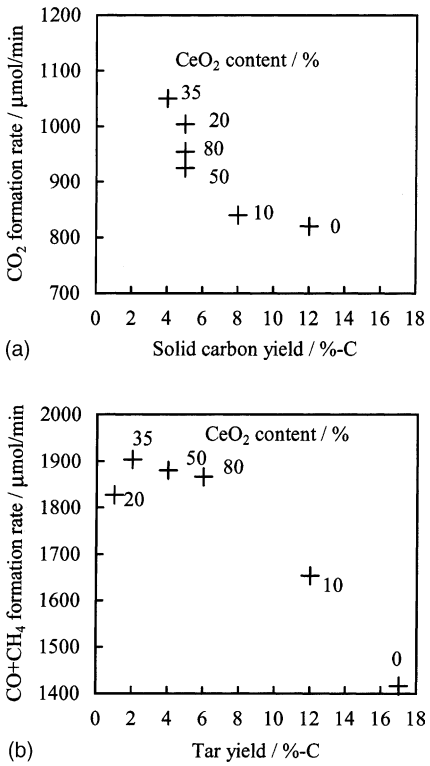

Fig. 4. Relation between the formation rate of products and the amount of solid carbon (a) and tar (b) in the gasification of cellulose over $Rh/CeO_2/SiO_2$ with various CeO_2 content using single-bed reactor. Reaction conditions are the same in Table 2.

part. In the lower part of the reactor, the catalyst surface is oxidized and it can contribute to the combustion of the pyrolyzed products including tar and solid carbon to form CO_2 and H_2O. On the other hand, some catalysts interacted with tar quickly move up by the fluidization and the catalyst becomes reduced at the upper part where the tar mainly takes part in the reforming reaction in the presence of steam on the catalyst surface to form CO and H_2, since the reactivity of solid carbon is low and the interaction between solid carbon and catalyst particles is weak. It is thought that solid carbon can react with oxygen in the lower part of the catalyst bed when it comes to the part.

It should be noted that much larger amount of solid carbon was formed in the case that the catalyst fluidization was not enough [45]. Therefore the fluidization is very important for the stable operation. It has been reported that the fluidized bed reactor is very effective to remove the low reactive carbonaceous species in the methane reforming with CO_2 and O_2 [58–61], which is serious problem in CO_2 reforming of methane [62–65].

As discussed above, the catalyst has to contribute to combustion under oxidative atmosphere and reforming under reductive atmosphere. This is also supported by our previous reports that commercial steam reforming Ni catalyst deactivated much more rapidly due to large amount of carbon deposition because the combustion activity of methane is much lower than $Rh/CeO_2/SiO_2$ [44]. This suggests that high combustion activity is important for the catalyst stability. From these considerations, it is expected that the role of CeO_2 can enhance both reforming and combustion activity, furthermore, the smooth redox properties in the combination of Rh and CeO_2 can match the fluidization [66].

3.2. Performance of real biomass gasification over $Rh/CeO_2/SiO_2$

One main component of real biomass is cellulose, however, wood biomass contains hemicellolose, lignin, and impurities such as sulfur, nitrogen and halogen. Therefore, it is more practical to test the performance of $Rh/CeO_2/SiO_2$ catalyst using the biomass such as cedar wood. Here, we used the $Rh/CeO_2/SiO_2(60)$ catalyst. From the optimization of CeO_2 content using cellulose as shown above, it is concluded that $Rh/CeO_2/SiO_2(35)$ is best. However, we also carried out the optimization using cedar wood, and we obtained the result that the best content was 60 mass% of CeO_2 although the detail is not shown here.

Fig. 5 shows the product distribution and C-conversion on $Rh/CeO_2/SiO_2(60)$ (a) and commercial steam reforming

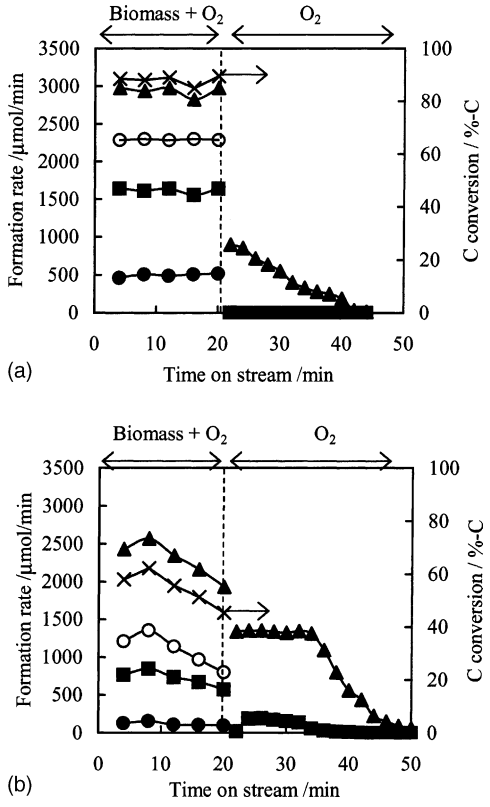

Fig. 5. Effect of time on stream on the carbon conversion and product distribution on (a) $Rh/CeO_2/SiO_2(60)$ and (b) G-91 in the gasification of cedar wood using single-bed reactor: (×) C-conversion, (○) H_2, (■) CO, (▲) CO_2, (●) CH_4. Catalyst 3 g, biomass 150 mg/min (H_2O 10%, C 5748 μmol/min; total H_2 4815 μmol/min; total O_2 2208 μmol/min), supplied O_2 42 ml/min (1719 μmol/min) from the bottom, ER = 0.28, N_2 68 ml/min (2782 μmol/min) from the bottom, N_2 60 ml/min (2455 μmol/min) from the top, and temperature 823 K.

Table 3
Comparison of the performance of various catalysts at different temperatures in the gasification of cedar wood

	T (K)	Formation rate (μmol/min)					H_2/CO	C-conversion (% C)	Solid carbon yield (% C)	Tar yield (% C)	Cold gas efficiency (%)
		CO	H_2	CO_2	CH_4	C_2					
$Rh/CeO_2/SiO_2(60)$	823	1605	2290	2915	513	–	1.4	88	11	1	55
	873	2093	2616	2744	785	–	1.3	97	3	0	71
	923	2594	3209	2497	628	–	1.2	99	1	0	77
	973	3024	3456	2109	580	–	1.1	99	1	0	82
G-91	823	747	1094	2255	116	–	1.5	54	34	12	22
	873	1464	1960	2497	219	–	1.3	73	15	12	41
	923	1963	2522	2329	245	–	1.3	79	10	11	52
	973	2562	3433	2252	309	–	1.3	89	9	2	69
Dolomite	823	566	174	1738	125	27	0.3	43	20	37	12
	873	731	248	1767	173	65	0.3	48	19	33	17
	923	1423	649	2533	270	99	0.5	75	17	8	32
	973	2017	1098	2474	461	180	0.6	89	9	2	50
	1073	2061	1335	2631	527	203	0.7	94	5	1	56
	1173	2403	1566	1939	580	480	0.7	94	5	3	70
Non-catalyst	823	549	132	1654	106	38	0.2	41	8	51	11
	873	849	169	1989	157	119	0.2	54	4	42	18
	923	1068	253	2037	213	150	0.2	60	3	36	24
	973	1288	338	2084	269	183	0.3	67	2	31	29
	1073	1890	603	2102	433	384	0.3	84	4	13	49
	1173	2268	732	2104	414	346	0.3	89	4	7	52

Conditions: catalyst 3 g, ER = 0.28, feeding rate 150 mg/min (10% moisture, C 5748 μmol/min, total H_2 4815 μmol/min and O_2 2208 μmol/min), N_2 flow 60 ml/min from the top and 68 ml/min from the bottom, O_2 flow 42 ml/min from the bottom. Cold gas efficiency is calculated by neglecting external heating [52].

catalyst G-91 (b) as a function of time on stream. The stability of the C-conversion and product distribution is one of the most important factors in the gasification process and it is available on $Rh/CeO_2/SiO_2(60)$ catalyst. On the other hand, the severe deactivation was observed over G-91. The details of the activity test using various methods are listed in Table 3. The C-conversion over $Rh/CeO_2/SiO_2$ was within 97–99% level above 873 K and thus the amount of the solid carbon was very low and no tar formation was observed. On the other hand, on G-91 catalyst, the C-conversion was below 90% level even at 973 K, and high yield of solid carbon and considerable yield of tar were observed. Considering the deactivation of G-91, $Rh/CeO_2/SiO_2$ showed much higher performance than G-91.

Table 3 also shows the comparison of the performance in the cedar gasification between $Rh/CeO_2/SiO_2(60)$ and conventional systems. On $Rh/CeO_2/SiO_2(60)$ catalyst the C-conversion is 88% at 823 K, which jumped to the 97% level at 873 K. Since the amount of char on $Rh/CeO_2/SiO_2(60)$ catalyst was very small even at lower temperature, the catalyst surface was kept quite clean and thus no deactivation was observed during the reaction period. On the other hand, the C-conversion is 43 and 41% on the dolomite catalyst and in the non-catalyzed systems, respectively at 823 K. Although the C-conversion attains to about 94% at high temperature (1173 K) on dolomite, the value is under 90% in the non-catalyzed system at the same temperature. The rest of the carbon in biomass related to the tar and solid carbon (Table 3) which is either deposited on the catalyst surface or exited the reactor with the flow of product gas. Fig. 6 shows the dependence of cold gas efficiency on reaction temperature using various methods. It is clear that the gasification of cedar wood over $Rh/CeO_2/SiO_2$ was more energy efficient than other methods. The efficiency over G-91 is apparently high, however, it is expected that the efficiency decreased with time on stream. In the case of non-catalyst and dolomite, high temperature is necessary for high efficiency.

The catalyst life in this biomass gasification process with 150 mg/min of feeding rate, 3 g of catalyst, ER around 0.3, and the oxygen supply in part of cocurrent and part

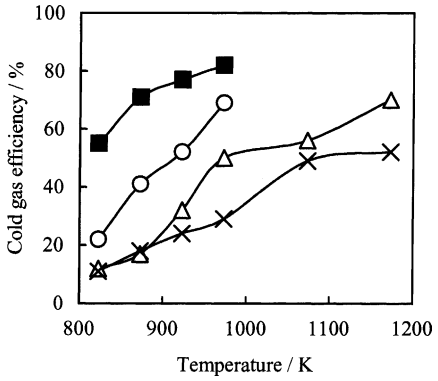

Fig. 6. Temperature dependence of cold gas efficiency using various methods in the gasification of cedar wood using single-bed reactor: (■) $Rh/CeO_2/SiO_2(60)$, (○) G-91, (△) dolomite, (×) non-catalyst. Reaction conditions are the same in Table 3.

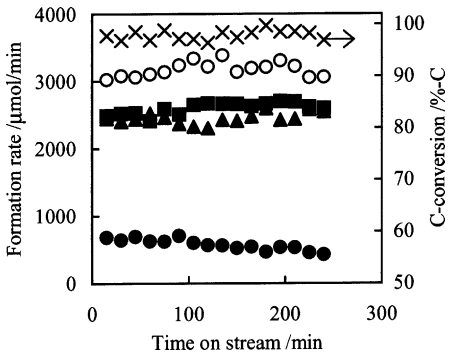

Fig. 7. Effect of time on stream on the carbon conversion and product distribution on (a) $Rh/CeO_2/SiO_2(60)$ and (b) G-91 in the gasification of cedar wood using single-bed reactor: (×) C-conversion, (○) H_2, (■) CO, (▲) CO_2, (●) CH_4. Catalyst 3 g, biomass 150 mg/min (H_2O 10%, C 5748 μmol/min; total H_2 4815 μmol/min; total O_2 2208 μmol/min), O_2 flow 21 ml/min (O_2 859 μmol/min) from the bottom, O_2 flow 21 ml/min (O_2 859 μmol/min) from the top, N_2 60 ml/min from the top, and 68 ml/min from the bottom, temperature 923 K [52].

of countercurrent systems at 923 K was tested for 4 h as shown in Fig. 7. The C-conversion was quite constant in the 98–99% level during the reaction period. The formation of CO, CO_2, and H_2 was almost stable with a subtle fluctuation may be due to the feeding rate fluctuation or experimental error. However, the formation of methane slowly decreased after about 2 h. The catalyst deactivation is mainly related to the solid carbon deposition on the catalyst surface and it was not severe problem in the case of our novel catalyst. Furthermore, the sulfur (0.02 mass%) and chlorine (0.01 mass%) present in the cedar wood are poisonous component for metal catalysts and they are supposed to deactivate the catalyst in this system. In the life test experiment, the total fed biomass was 36 g on 3 g of catalyst. The sulfur and chlorine in the fed biomass were estimated to be 0.23 and 0.10 mmol, respectively. According to the hydrogen chemisorption, the dispersion of Rh (H/Rh = 0.16), about 0.058 mmol of Rh presents on the 3 g of catalyst surface, which is much lower amount than the fed sulfur and chlorine. However, almost no deactivation of the catalyst was observed during the reaction period. This suggests that the sulfur and chlorine adsorbed on the catalyst surface can easily removed by oxidation or reduction activities of the catalyst in the fluidized bed reactor [52]. Further investigation on effect of poisonous materials is necessary for the elucidation of the mechanism of their removal from the catalyst surface.

3.3. *Pyrogasification and steam reforming of cedar wood using $Rh/CeO_2/SiO_2$ and conventional methods*

It is found that $Rh/CeO_2/SiO_2(60)$ exhibited much higher performance and gave much more energy efficient than the conventional methods (non-catalyst, dolomite, commercial steam reforming catalyst) in the gasification of cedar wood with air using single-bed reactor as shown above. Here, we also have tested the performance in the pyrogasification and steam reforming of cedar using $Rh/CeO_2/SiO_2$ and conventional methods.

Catalytic performance in the pyrogasification of cedar over G-91 and $Rh/CeO_2/SiO_2(60)$ as well as non-catalyst and dolomite is listed in Table 4. In addition, Fig. 8 shows reaction temperature dependence of the carbon-based yield of the products. In the case of non-catalyst, mainly tar was formed as shown in Fig. 8(a). When dolomite was used, tar

Table 4
Performance of various catalysts in the pyrogasification of cedar wood

Catalyst	T (K)	Formation rate (μmol/min)					H_2/CO
		CO	H_2	CH_4	C_2[a]	CO_2	
None	873	408	152	92	81	150	0.4
	923	530	250	116	120	239	0.4
	973	636	220	153	145	244	0.3
	1023	616	264	232	215	305	0.4
Dolomite	873	375	160	141	55	185	0.4
	923	528	316	137	74	299	0.6
	973	604	432	147	86	374	0.7
	1023	697	526	237	148	314	0.8
G-91	873	690	985	244	–	375	1.4
	923	750	1116	237	–	365	1.5
	973	1071	1300	227	–	333	1.2
	1023	1329	1367	194	–	272	1.0
$Rh/CeO_2/SiO_2(60)$	873	961	1270	290	–	368	1.3
	923	1107	1313	348	–	364	1.2
	973	1285	1314	321	–	339	1.0
	1023	1592	1467	328	–	227	0.9

Conditions: catalyst 3 g, biomass 60 mg/min (H_2O 10%, C, 2299 μmol/min; H, 3185 μmol/min; O, 1767 μmol/min), N_2 25 ml/min from the top and 25 ml/min from the bottom (total 2046 μmol/min) [55].

[a] Carbon based.

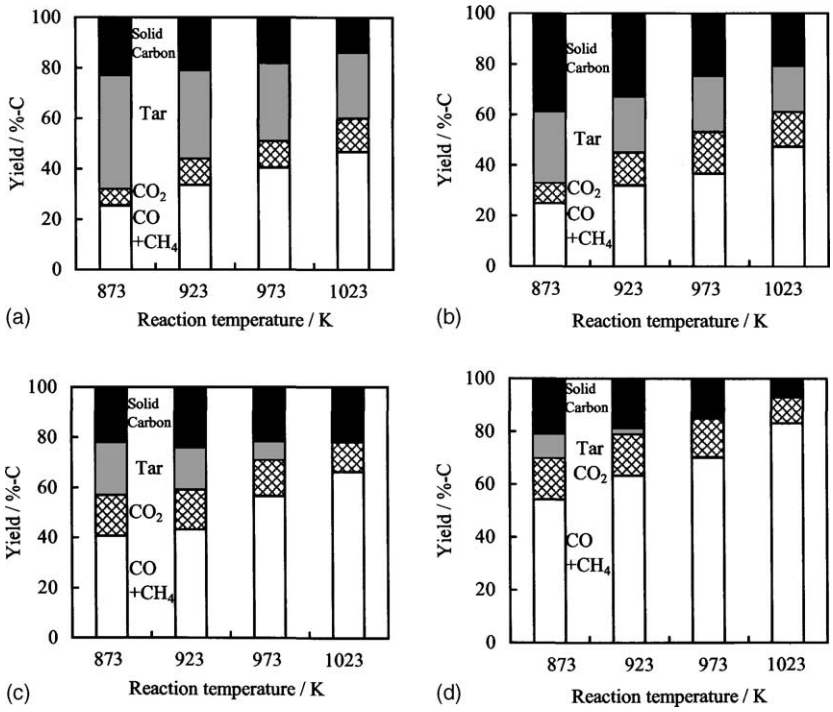

Fig. 8. Temperature dependence of the distribution of carbon containing products in pyrogasification of cedar wood using the single-bed reactor. (a) Non-catalyst, (b) dolomite, (c) G-91, (b) $Rh/CeO_2/SiO_2(60)$. Conditions: catalyst 3 g, biomass 60 mg/min (H_2O 10%, C 2299 μmol/min; H 3185 μmol/min; O 1767 μmol/min), N_2 25 ml/min from the top and 25 ml/min from the bottom (total 2046 μmol/min). In the case of non-catalyst and dolomite, $CO + CH_4$ included C_2 [55].

yield decreased and at the same time the yield of solid carbon increased. This indicates that cracking of tar to solid carbon can proceed on dolomite. It is characteristic that the yield of solid carbon was almost the same at various reaction temperatures over G-91 as shown in Fig. 8(c). The yield of tar drastically decreased and gas yield increased by using G-91 compared to non-catalyst. However, solid carbon yield on G-91 was higher than that on non-catalyst, especially at higher reaction temperature. This can be due to the conversion of a part of tar and gas to solid carbon via dehydrogenation reaction and CO disproportionation. In contrast, $Rh/CeO_2/SiO_2(60)$ decreased the yield of solid carbon and tar drastically, and then increased the yield of $CO + CH_4$. The yield of solid carbon was lower than that on non-catalyst, and this suggests that inert solid carbon can be converted over $Rh/CeO_2/SiO_2$. In this system, since oxygen is not introduced at all, it is expected that carbon reacts with steam, and $Rh/CeO_2/SiO_2$ can catalyze the reaction of solid carbon with steam. However, the interaction between $Rh/CeO_2/SiO_2$ and the solid carbon may be weak, and the reaction mechanism is not clear at present. In addition, the yield of tar over $Rh/CeO_2/SiO_2$ was much lower than that over G-91. In the pyrogasification, steam is present and is formed from the biomass pyrolysis although the partial pressure of steam is low. Therefore the reforming of tar with this steam occurs. The result indicates that the activity of tar reforming over $Rh/CeO_2/SiO_2$ was much higher than that over G-91.

Catalytic performance in the steam reforming of cedar wood over G-91 and $Rh/CeO_2/SiO_2(60)$ is listed in Table 5. In addition, Fig. 9 shows reaction temperature dependence of the carbon-based yield of the products. In the case of G-91, the yield of solid carbon decreased with increasing reaction temperature. This behavior is much different from that in the pyrogasification. The yield of tar also decreased with the reaction temperature. The effect of $Rh/CeO_2/SiO_2(60)$ was much more drastic. The yield of solid carbon and tar was much lower than that in the pyrogasification. The tar yield became zero at 973 K. This indicates that steam can promote the gasification of cedar wood via reforming reaction. In addition, compared with pyrogasification, CO formation became lower and H_2/CO ratio drastically increased by the addition of steam via water gas shift reaction ($CO + H_2 \rightarrow CO_2 + H_2$).

3.4. Comparison between single-bed and dual-bed reactors in the gasification of cedar wood

We compared the performance in the gasification of cedar wood using the single-bed and dual-bed reactors as summarized in Table 6. In the single-bed reactor, all the components in the biomass contacted with catalyst and oxygen. Thus, there is a possibility of complete C-conversion to gas. Consequently, C-conversion in the single-bed system was around 98% at 873 K. In contrast, in the dual-bed system, only tar and other volatile matter can be contacted with

Table 5
Catalyst performance in the steam reforming of cedar wood in the single-bed reactor

Catalyst	T (K)	Steam flow rate (μmol/min)	Formation rate (μmol/min)				H_2/CO
			CO	H_2	CH_4	CO_2	
G-91	823	1666	144	2493	204	1232	17.3
	873	1666	306	2502	234	1068	8.2
	923	1666	373	2448	158	1313	6.6
	973	1666	553	2807	86	1253	5.1
$Rh/CeO_2/SiO_2(60)$	823	1666	210	2003	446	1215	9.5
	873	1666	166	1942	555	1208	11.7
	923	1666	340	1931	587	1227	5.7
	973	1666	450	1884	433	1291	4.2

Conditions: catalyst 3 g, biomass 60 mg/min (H_2O 10%, C, 2299 μmol/min; H, 3185 μmol/min; O, 1767 μmol/min), N_2 25 ml/min from the top and 25 ml/min from the bottom (total 2046 μmol/min) [55].

catalyst particles and oxygen. Thus, the C-conversion in the dual-bed reactor was usually around 80% in temperature range of 823–923 K. In the catalytic gasification reaction, the solid carbon (char and coke) forms in two ways; one is formed directly from biomass during the pyrolysis, and this is called as char. The other one is formed during the tar reforming on the catalyst surface, and this is called as coke. In the single-bed systems, these two types of solid carbon cannot be measured separately by burning them together after the activity test. However, in the dual-bed system, these can be measured separately and the results are listed in Table 6. The rest of the carbon (about 20%) was accumulated as char in the primary-bed which are formed by the pyrolysis of cedar wood. A small fraction of tar was converted in to coke (1.5–0.5% C), which was deposited on the catalyst surface. It is concluded that the dual-bed reactor gave higher yield of useful product gases (CO, H_2 and CH_4) than single-bed system, especially at lower reaction temperature. As mentioned in previous section, the catalyst with higher combustion and reforming activities exhibited higher performance in the gasification using single-bed reactor. This is because the deposited carbon should be removed by combustion. In contrast, in the dual-bed reactor, there is no interaction between the catalyst and char with low reactivity. Therefore, the amount of carbon on the catalyst is reduced and it is expected that the stability is enhanced even on the catalyst with low combustion activity.

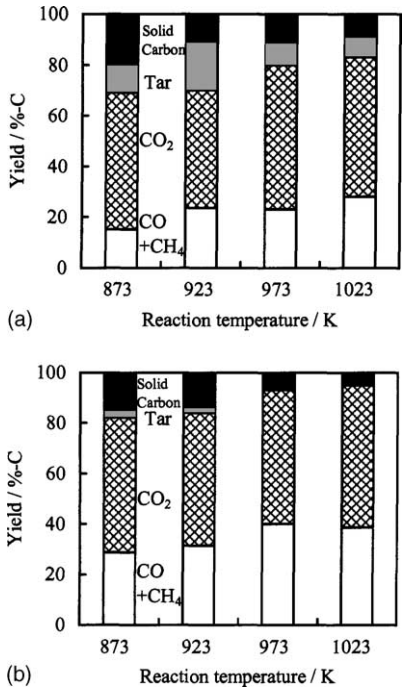

Fig. 9. Temperature dependence of the distribution of carbon containing products in steam reforming of cedar wood in the single-bed reactor. (a) G-91, (b) $Rh/CeO_2/SiO_2(60)$. Conditions: catalyst 3 g, biomass 60 mg/min (H_2O 10%, C 2299 μmol/min; H 3185 μmol/min; O 1767 μmol/min), N_2 25 ml/min from the top and 25 ml/min from the bottom (total 2046 μmol/min), H_2O 1666 μmol/min from the bottom [55].

3.5. Comparison between CeO_2/SiO_2 supported noble metals and nickel catalysts in dual-bed reactors

The catalysts used in this investigation are $M/CeO_2/SiO_2$ (M = Rh, Pd, Pt, Ru, Ni) with 1.2×10^{-4} mol/g_{cat}. Metals (Rh, Pd, Pt, Ru) were loaded on CeO_2/SiO_2 by impregnation of the support with acetone solution of $Rh(C_5H_7O_2)_3$, $Pd(C_5H_7O_2)_2$, $Pt(C_5H_7O_2)_2$, $Ru(C_5H_7O_2)_3$, respectively. In the case of $Ni/CeO_2/SiO_2$, $Ni(NO_3)_2{\cdot}6H_2O$ aqueous solution was used. The calcination at 773 K for 3 h was carried out after the drying at 383 K for 12 h. In each run of the activity test, 3 g of catalyst was used and pretreated by hydrogen flow at 773 K for 0.5 h.

For the comparison of the performance of various catalysts, the formation rate of $CO + H_2 + CH_4$ over various catalysts are shown in Fig. 10. The details of the results are listed in Table 7. The order of the activity at 823 K in the gasification of cedar wood to synthesis gas was as follows: Rh > Pd > Pt > Ni = Ru. In the case of Ru, the activity at 923 K also the lowest. On the other hand, the activity of Ni at 923 K becomes higher than that over Pd(Rh > Pt = Pd = Ni > Ru). This indicates that $Ni/CeO_2/SiO_2$ catalyst can give high performance at high temperature. In contrast, $Rh/CeO_2/SiO_2$ exhibited higher performance in the range of 823–923 K. In addition, the results of H_2 chemisorption

Table 6
Comparison of the performance of $Rh/CeO_2/SiO_2(60)$ in the single-bed and dual-bed systems for the gasification of cedar wood

Reactor	T (K)	Formation rate (μmol/min)					C-conversion (% C)	Char yield (% C)	Coke yield (% C)	Tar yield (% C)
		CO	H_2	CO_2	CH_4	$CO + H_2 + CH_4$				
Single-bed	823	1605	2290	2914	512	4407	88	12.0[a]	–	0
	873	2093	2615	2743	784	5492	98	2.0[a]	–	0
	923	2593	3208	2496	628	6429	99	1.0[a]	–	0
	973	3024	3456	2109	580	7060	99	1.0[a]	–	0
Dual-bed	823	2077	2638	1961	467	5182	78	720.5	1.5	0
	873	2091	3079	1959	363	5533	77	22.0	1.0	0
	923	2784	3666	1492	213	6663	78	21.5	0.5	0

Conditions: catalyst 3 g, biomass 150 mg/min (H_2O 10%, C 5748 μmol/min, total H_2 4815 μmol/min and total O_2 2208 μmol/min), supplied O_2 35 ml/min (1432 μmol/min), N_2 150 ml/min (6138 μmol/min) and ER = 0.25.

[a] Char + coke (solid carbon): it is difficult to determine separately in single-bed reactor. SiO_2 support: Aerosil 380 (380 m^2/g).

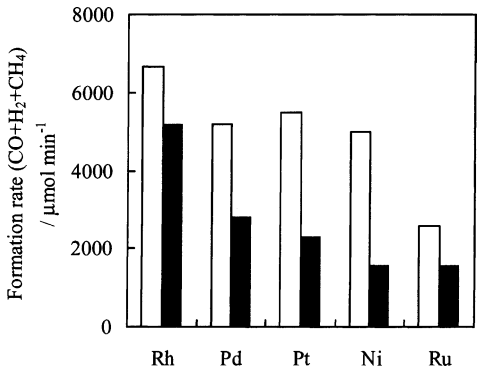

Fig. 10. Comparison of $M/CeO_2/SiO_2$ catalysts (M = Rh, Pd, Pt, Ru, Ni) in the gasification of cedar wood using the dual-bed reactor. Formation rate of $CO + H_2 + CH_4$: open bar 923 K, filled bar 823 K. Reaction conditions: catalyst 3 g, biomass 150 mg/min (H_2O 10%, C 5748 μmol/min; total H_2 4815 μmol/min; total O_2 2208 μmol/min), supplied O_2 35 ml/min (1432 μmol/min), ER = 0.25, total N_2 150 ml/min (6138 μmol/min).

are also shown in Table 7. Furthermore, H/M and BET surface area of $Rh/CeO_2/SiO_2$ were determined to be 0.16 and 125 m^2/g, respectively. It is found that the H/M molar ratio on Rh catalyst was almost the same level as that of other catalysts. This indicates that the activity is not determined by high metal dispersion, and the properties of metal influenced the performance. It is suggested that the activity in the gasification of cedar wood using the dual-bed reactor is related to that in reforming of hydrocarbons. On the other hand, the low activity over Ru catalyst can be due to the loss of Ru metal from the catalyst surface, which is caused by the oxidation of Ru to volatile Ru oxide. In addition, the performance can be reflected by the difference in the resistance to poisoning with S and Cl. It is necessary to investigate the effect of poisonous materials such as S and Cl on the gasification performance in the future.

Table 7
Catalyst properties and performance in the gasification of cedar wood over $M/CeO_2/SiO_2$ using the dual-bed reactor

Metal	T (K)	Formation rate (μmol/min)								Characterization	
		CO	H_2	CH_4	CO_2	C-conversion (% C)	Char yield (% C)	Coke yield (% C)	Tar yield (% C)	H_2 adsorption, H/M (mol/mol)	BET (m^2/g)
Pt	823	890	1217	193	1647	48	31	5	16	0.21	128
	873	1475	2211	268	2023	66	27	2	5		
	923	2234	3171	85	2018	76	23	1	0		
Pd	823	1488	1049	258	1437	55	30	5	10	0.14	127
	873	1830	2347	226	1944	69	24	2	5		
	923	2287	2834	82	1802	73	23	2	2		
Ru	823	841	579	159	1604	45	32	6	17	–	–
	873	1139	1111	263	2079	61	30	3	6		
	923	1433	764	388	1459	57	30	3	10		
Ni	823	827	579	154	1907	50	36	3	11	0.05	136
	873	1454	993	299	1821	64	27	2	7		
	923	2096	2542	339	1726	73	24	2	1		

$M/CeO_2/SiO_2$: loading of M = 1.2×10^{-4} mol/g_{cat}, loading of CeO_2 = 60 mass%. Reaction conditions: catalyst 3.0 g, biomass 150 mg/min (H_2O 10 mass%, C 5748 μmol/min, total H_2 4815 μmol/min, total O_2 2208 μmol/min), supplied O_2 35 ml/min (1432 μmol/min), ER = 0.25, total N_2 150 ml/min (6138 μmol/min).

3.6. The gasification of rice straw in the single-bed and dual-bed reactors

In the fluidized-bed reactor, the physical strength of the catalyst particles is very important. This is because the attrition rate is considerably high when the physical strength of catalyst is low. $Rh/CeO_2/SiO_2$ particles used above were prepared by pressing fine powders of SiO_2 (Aerosil 380). And then we observed the attrition of the catalyst particles, especially in the activity test for longer time on stream. Therefore the catalysts with higher physical strength are favorable, and we applied the commercial SiO_2 granules: CARiACT G-6 (size 0.18–0.50 mm, BET = 535 m^2/g) supplied from Fuji Silysia Chemical Ltd. This support exhibited highest performance among some supports which we have tested. The loading of CeO_2 and Rh on SiO_2(G-6) was carried out in the same way as that on powder SiO_2.

Fig. 11 shows the effect of time on stream on C-conversion and product distribution for the gasification of rice straw over $Rh/CeO_2/SiO_2$(G-6)(30) in the single-bed and dual-bed reactors. The CeO_2 content was optimized from the activity test although the details are not shown here. In the case of the single-bed reactor, the rapid deactivation was observed. It should be noted that the deactivation of H_2 formation was more rapid than CO and CO_2. In fact, since C-conversion was almost the same during the reaction, it can be interpreted that the reforming of tar to CO and H_2 is suppressed and the conversion to CO and H_2O proceeds. Although the details are not clear at present, the non-catalytic gasification can give similar behavior as shown in Table 3. In the case of the gasification of cedar wood on non-catalyst, H_2/CO ratio was much lower compared to $Rh/CeO_2/SiO_2$. In addition, the deactivation was not observed at all in the gasification of cedar wood when $Rh/CeO_2/SiO_2$ catalyst was used. On the other hand, it is found that the dual-bed reactor inhibited the catalyst deactivation significantly (Fig. 11(b)).

There are some possible reasons for the catalyst deactivation. As listed in Table 1, rice straw contains much larger amount of ash than other biomass (cedar wood, jute stick and baggase). This suggests that the ash can cause the catalyst deactivation. At present, we have not analyzed the component of ash in rice straw in detail yet. In order to elucidate the deactivation mechanism, further investigation on the analysis of ash and spent catalyst is necessary. In addition, it is characteristic that the ratio of fixed carbon of

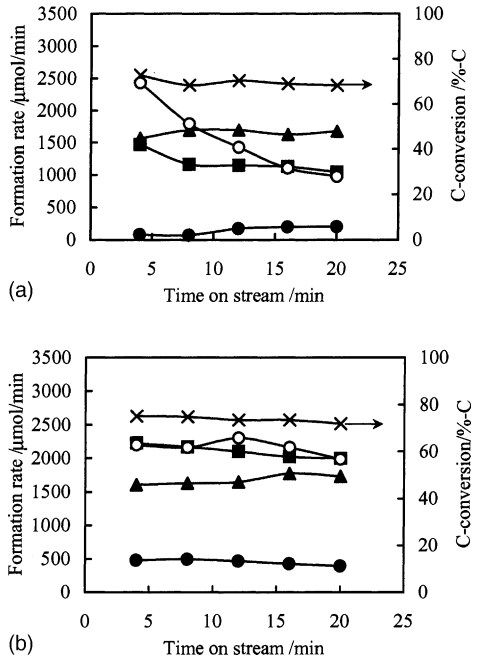

Fig. 11. Effect of time on stream on C-conversion and product distribution for the gasification of rice straw over $Rh/CeO_2/SiO_2$(G-6)(30). (a) Single-bed reactor, (b) dual-bed reactor: (×) C-conversion, (○) H_2, (■) CO, (▲) CO_2, (●) CH_4. Catalyst 3 g, feeding rate: 200 mg/min, supplied O_2 35 ml/min (1432 μmol/min), ER = 0.25, N_2 150 ml/min (6138 μmol/min) and temperature 873 K.

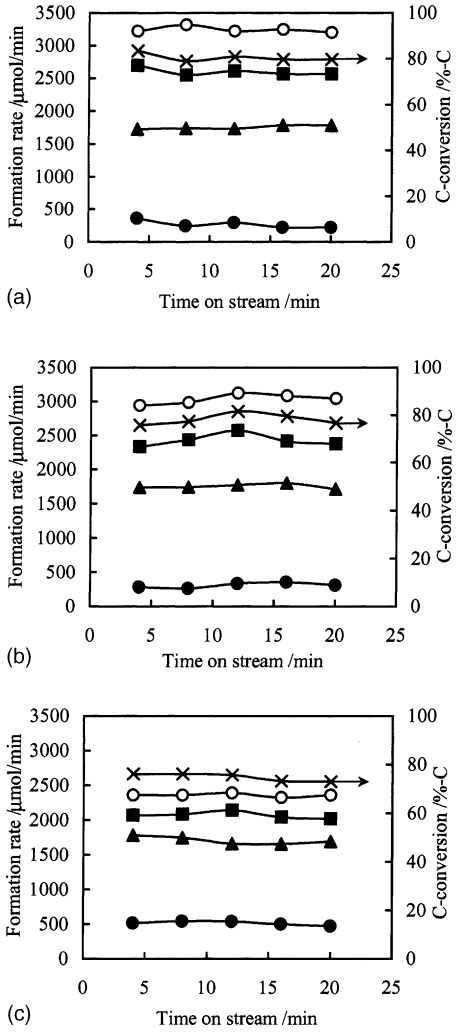

Fig. 12. Effect of time on stream on C-conversion and product distribution for the gasification of various biomasses over $Rh/CeO_2/SiO_2$(G-6)(30) in the dual-bed reactor. (a) Cedar wood, (b) jute stick, (c) baggase: (×) C-conversion, (○) H_2, (■) CO, (▲) CO_2, (●) CH_4. Catalyst 3 g, feeding rate: 200 mg/min, supplied O_2 35 ml/min (1432 μmol/min), ER = 0.25, N_2 150 ml/min (6138 μmol/min) and temperature 873 K.

Table 8
Effect of temperature on the gasification of various biomass on $Rh/CeO_2/SiO_2$(G-6)(30) catalyst

Biomass	T (K)	Formation rate (μmol/min)				H_2/CO	C-conversion (% C)	Char yield (% C)	Coke yield (% C)	Tar yield (% C)
		CO	H_2	CO_2	CH_4					
Cedar	823	2152	2686	1841	517	1.3	78	20.8	1.2	0
	873	2599	3232	1752	269	1.2	80	19.1	0.8	0
	923	2902	3541	1605	148	1.2	81	18.5	0.5	0
Jute	823	2032	2634	1729	323	1.3	71	24.0	3.0	2.0
	873	2362	3036	1818	306	1.3	78	17.0	1.0	0.0
	923	3057	3255	1577	218	1.1	84	14.5	0.5	0.0
Baggase	823	1850	2057	1645	416	1.1	68	21.0	4.0	7.0
	873	2050	2357	1739	516	1.2	75	21.0	2.0	2.0
	923	2965	3264	1587	205	1.1	82	17.0	1.0	0.0
Rice straw	823	1797	2057	1569	366	1.2	65	21.0	4.0	10.0
	873	2102	2162	1677	452	1	74	19.0	4.0	3.0
	923	2878	3167	1524	172	1.1	80	16.0	2.0	2.0

Conditions: catalyst 3 g, ER = 0.24, feeding rate of cedar, jute stick, baggase 150 mg/min (moisture: cedar 10%, jute stick 3%, baggase 5%) and rice straw 200 mg/min (moisture 5%, C 35%). N_2 flow 100 ml/min through the feeding line and 50 ml/min from the top, O_2 flow 35 ml/min through the catalyst bed.

rice straw was higher than that of others. This suggests that the character of char of rice straw is different from that of others. Larger retention of char from the rice straw in the catalyst bed can decrease the activity in the single-bed reactors. In the case of the single-bed reactor, the ash and char must contact with the catalyst surface during the reaction time. In contrast, in the case of the dual-bed reactor, the ash and char was accumulated in the primary-bed, and it cannot contact with the catalyst. This can explain the difference between the single-bed and dual-bed reactors.

Fig. 12 shows the effect of time on stream on C-conversion and product distribution for the gasification of different biomasses over $Rh/CeO_2/SiO_2$(G-6)(30) in dual-bed reactors. The details of the results are listed in Table 8. When we used the dual-bed reactor, the stable activity in the gasification of four biomasses was observed during the 20 min reaction. However, the performance was dependent on the kind of biomasses. The order of the syngas yield was as follows: cedar > jute > baggase > rice straw. In terms of the impurities such as nitrogen, chloride, sulfur, and ash, the order of the amount is as follows: cedar > jute > baggase > rice straw (Table 1). This order agrees with that of the syngas yield. This correspondence suggests the impurities can affect the catalyst performance. However, the mechanism of impurity effect is unclear at present. The investigation on the effect of impurities is necessary in the future.

4. Conclusions

1. It is found that $Rh/CeO_2/SiO_2$ gave higher energy efficiency than the conventional methods (non-catalyst, dolomite, and commercial steam reforming Ni catalyst) in cedar gasification using single-bed fluidized bed reactor.
2. From the results of the effect of CeO_2 amount in $Rh/CeO_2/SiO_2$ in the gasification of cellulose it is suggested that CeO_2 plays an important role in promoting combustion activity and reforming activity.
3. $Rh/CeO_2/SiO_2$ also showed higher performance in the pyrogasification and steam reforming of cedar wood than the commercial steam reforming Ni catalysts.
4. In the gasification of cedar wood on $Rh/CeO_2/SiO_2$ catalyst, the yield of synthesis gas using the dual-bed reactor was higher than that using the single-bed reactor.
5. On CeO_2/SiO_2 supported noble metal catalysts in the dual-bed reactor, the order of the gasification performance was as follows: Rh > Pt > Pd > Ni = Ru, and it is concluded that Rh is an effective component.
6. In the gasification of rice straw using the single-bed reactor over $Rh/CeO_2/SiO_2$, the rapid deactivation was observed probably because of high ash content and fixed carbon ratio in the rice straw. In contrast, the dual-bed reactor inhibited the catalyst deactivation drastically.
7. It is found that the combination of $Rh/CeO_2/SiO_2$ with the fluidized dual-bed reactor is effective for the gasification of cedar wood, jute stick, baggase, and rice straw at lower temperature than usual.

Acknowledgements

This research was supported by the Future Program of Japan Society for the Promotion of Sciences under the Project “Synthesis of Ecological High Quality of Transportation Fuels” (JSPS-RFTF98P01001).

References

[1] M. Yamada, Energy and Fuels 17 (2003) 797.
[2] J.M. Ogden, Annu. Rev. Energy Environ. 24 (1999) 227.
[3] M.A. Caballero, J. Corella, M.P. Aznar, J. Gil, Ind. Eng. Chem. Res. 39 (2000) 1143.

[4] F. Miccio, O. Moersch, H. Spliethoff, K.R.G. Hein, Fuel 78 (1999) 1473.
[5] C. Brage, Q. Yu, G. Chen, K. Sjostrom, Biomass and Bioenergy 18 (2000) 87.
[6] I. Narváez, A. Orío, M.P. Aznar, J. Corella, Ind. Eng. Chem. Res. 35 (1996) 2110.
[7] P. Vriesman, E. Heginuz, K. Sjöström, Fuel 79 (2000) 1371.
[8] C.D. Blasi, G. Signorelli, G. Portoricco, Ind. Eng. Chem. Res. 38 (1999) 2571.
[9] J. Gil, M.P. Aznar, M.A. Caballero, E. Francés, J. Corella, Energy and Fuels 11 (1997) 1109.
[10] A.A.C.M. Beenackers, Renewable Energy 16 (1999) 1180.
[11] F. Miccio, O. Moersch, H. Spliethoff, K.R.G. Hein, Fuel 78 (1999) 1473.
[12] K. Maniatis, A.A.C.M. Beenackers, Biomass and Bioenergy 18 (2000) 1.
[13] N. Abatzoglou, N. Barker, P. Hasler, H. Knoef, Biomass and Bioenergy 18 (2000) 5.
[14] H.A.M. Knoef, H.J. Koele, Biomass and Bioenergy 18 (2000) 55.
[15] S. Yokoyama (Ed.), Biomass Handbook, Japan Institute of Energy, 2002, p. 95.
[16] F. Engstrom, Biomass and Bioenergy 15 (1998) 259.
[17] D.N. Bangala, N. Abatzoglou, J.-P. Martin, E. Chornet, Ind. Eng. Chem. Res. 36 (1997) 4184.
[18] A. Olivares, M.P. Aznar, M.A. Caballero, J. Gil, E. Frances, J. Corella, Ind. Eng. Chem. Res. 36 (1997) 5220.
[19] L. Mudge, E.G. Baker, D.G. Mitchell, Investigations on Catalyzed Steam Gasification of Biomass, PNL-3695, Pacific Northwest National Laboratory, Richland, WA, 1981.
[20] C. Ekstrom, N. Lindman, R. Petterson, Catalytic conversion of tars, carbon black, and methane from pyrolysis/gasification of biomass, in: R.P. Overend, T.A. Milne, L.K. Mudge (Eds.), Proceedings of the Fundamentals of Thermochemical Conversion of Biomass Conference, Elsevier Applied Press, London, 1982, p. 601.
[21] A.A.C.M. Beenackers, K. Maniatis, Gas cleaning in electricity production via gasification of biomass, in: A.V. Bridgewater (Ed.), Proceedings of the Conclusions of the Workshop on Advances in Thermochemical Biomass Conversion, Blackie Academic Press, London, 1994, p. 540.
[22] A.V. Bridgwater, Appl. Catal. 116 (1994) 5.
[23] P. Simell, E. Kurkela, P. Ståhlberg, Formation and catalytic decomposition of tars from fluidized bed gasification, in: A.V. Bridgwater (Ed.), Advances in Thermochemical Biomass Conversion, Blackie Academic Press, London, 1994, p. 265.
[24] N. Abatzoglou, P. Legast, P. Delvaux, D. Bangala, E. Chornet, Gas conditioning technologies for biomass and waste gasification, in: R.P. Overend, E. Chornet (Eds.), Proceedings of the Third Biomass Conference of the Americas, Elsevier Science Ltd., Oxford, 1997, p. 599.
[25] M.P. Aznar, J. Corella, J. Gil, A. Martin, M.A. Caballero, A. Olivares, P. Perez, A.V. Bridgwater, D.G.B. Boocock (Eds.), Biomass Gasification with Steam and Oxygen Mixtures at Pilot Plant Scale and Catalytic Gas Upgrading. Part I. Developments in Thermochemical Biomass Conversion, Blackie Academic and Professional, London, 1997, p. 1194.
[26] T.A. Milne, N. Abatzoglou, R.J. Evans, Biomass Gasifier "Tars": Their Nature, Formation, and Conversion, NREL/TP-570-25357, National Renewable Energy Laboratory, Golden, CO, 1998.
[27] M.A. Caballlero, M.P. Aznar, J. Corella, J. Gil, J.A. Martin, in: R.P. Overend, E. Chornet (Eds.), Proceedings of the Fourth Biomass Conference of the Americas, Pergamon Press, Oxford, 1999, p. 979.
[28] J. Corella, M.A. Caballero, M.P. Aznar, J. Gil, in: R.P. Overend, E. Chornet (Eds.), Proceedings of the Fourth Biomass Conference of the Americas, Pergamon Press, Oxford, 1999, p. 933.
[29] D. Sutton, B. Kelleher, J.R.H. Ross, Fuel Process. Technol. 73 (2001) 155.
[30] L. García, M.L. Salvador, J. Arauzo, R. Bilbao, Energy and Fuels 13 (1999) 851.
[31] L. García, M.L. Salvador, J. Arauzo, R. Bilbao, Fuel Process. Technol. 69 (2001) 157.
[32] L. García, R. French, S. Czernik, E. Chornet, Appl. Catal. A: Gen. 201 (2000) 225.
[33] L. García, M.L. Salvador, J. Arauzo, R. Bilbao, Ind. Eng. Chem. Res. 37 (1998) 3812.
[34] J. Arauzo, D. Radlein, J. Piskorz, D.S. Scott, Ind. Eng. Chem. Res. 36 (1997) 67.
[35] J. Arauzo, D. Radlein, J. Piskorz, D.S. Scott, Energy and Fuels 8 (1994) 1192.
[36] C. Courson, E. Makaga, C. Petit, A. Kiennemann, Catal. Today 63 (2000) 427.
[37] Y. Tanaka, T. Yamaguchi, K. Yamasaki, A. Ueno, Y. Kotera, Ind. Eng. Chem. Res. 23 (1984) 225.
[38] J. Gil, M.A. Caballero, J.A. Martin, M.-P. Aznar, J. Corella, Ind. Eng. Chem. Res. 38 (1999) 4226.
[39] S. Rapagna, N. Jand, A. Kiennemann, P.U. Foscolo, Biomass and Bioenergy 19 (2000) 187.
[40] E.G. Baker, L.K. Mudge, M.D. Brown, Ind. Eng. Chem. Res. 26 (1987) 1335.
[41] E.G. Baker, L.K. Mudge, W.A. Wilcox, Catalysis of gas phase reactions in steam gasification of biomass, in: R.P. Overend, et al. (Eds.), Fundamentals of Thermochemical Biomass Conversion, Elsevier Applied Science, London, 1985, p. 863.
[42] M. Asadullah, K. Tomishige, K. Fujimoto, Catal. Commun. 2 (2001) 63.
[43] M. Asadullah, K. Tomishige, K. Fujimoto, Ind. Eng. Chem. Res. 25 (2001) 5894.
[44] M. Asadullah, S. Ito, K. Kunimori, M. Yamada, K. Tomishige, J. Catal. 208 (2002) 255.
[45] M. Asadullah, S. Ito, K. Kunimori, K. Tomishige, Ind. Eng. Chem. Res. 41 (2002) 4567.
[46] M. Asadullah, S. Ito, K. Kunimori, M. Yamada, K. Tomishige, Environ. Sci. Technol. 36 (2002) 4476.
[47] K. Tomishige, M. Asadullah, S. Ito, K. Kunimori, Kagaku Kogaku Ronbunshu 28 (2002) 666.
[48] K. Tomishige, M. Asadullah, S. Koyama, S. Ito, K. Kunimori, J. Jpn. Inst. Energy 82 (2003) 261.
[49] K. Tomishige, T. Miyazawa, M. Asadullah, S. Ito, K. Kunimori, J. Jpn. Petrol. Inst. 46 (2003) 69.
[50] M. Asadullah, T. Miyazawa, S. Ito, K. Kunimori, K. Tomishige, Stud. Surf. Sci. Catal. 145 (2003) 307.
[51] M. Asadullah, T. Miyazawa, S. Ito, K. Kunimori, M. Yamada, K. Tomishige, Green Chem. 4 (2002) 385.
[52] M. Asadullah, T. Miyazawa, S. Ito, K. Kunimori, K. Tomishige, Appl. Catal. A: Gen. 246 (2003) 103.
[53] K. Tomishige, M. Asadullah, K. Kunimori, Catal. Surv. Asia 7 (2003) 219.
[54] M. Asadullah, T. Miyazawa, S. Ito, K. Kunimori, K. Tomishige, Energy and Fuels 17 (2003) 542.
[55] K. Tomishige, T. Miyazawa, M. Asadullah, S. Ito, K. Kunimori, J. Jpn. Petrol. Inst. 46 (2003) 322.
[56] K. Tomishige, T. Miyazawa, M. Asadullah, S. Ito, K. Kunimori, Green Chem. 5 (2003) 399.
[57] M. Asadullah, T. Miyazawa, S. Ito, K. Kunimori, M. Yamada, K. Tomishige, Appl. Catal. A: Gen. 255 (2003) 169.
[58] K. Tomishige, Y. Matsuo, Y. Sekine, K. Fujimoto, Catal. Commun. 2 (2001) 11.
[59] K. Tomishige, Y. Matsuo, Y. Yoshinaga, Y. Sekine, M. Asadullah, K. Fujimoto, Appl. Catal. A: Gen. 223 (2002) 225.
[60] Y. Matsuo, Y. Yoshinaga, Y. Sekine, K. Tomishige, K. Fujimoto, Catal. Today 63 (2000) 439.

[61] K. Tomishige, Y. Matsuo, Y. Yoshinaga, M. Asadullah, Y. Sekine, K. Fujimoto, ACS Symp. Ser. 809 (2002) 303.
[62] K. Tomishige, Y. Chen, K. Fujimoto, J. Catal. 181 (1999) 91.
[63] K. Tomishige, K. Fujimoto, Catal. Surv. Jpn. 2 (1998) 3.
[64] K. Tomishige, K. Fujimoto, J. Jpn. Petrol. Inst. 44 (2001) 65.
[65] Y. Himeno, K. Tomishige, K. Fujimoto, J. Jpn. Petrol. Inst. 42 (1999) 252.
[66] A. Trovarelli, Catal. Rev. 38 (1996) 439.